Journal of Orthopaedic Translation 26 (2021) 141–150

Contents lists available at ScienceDirect

Journal of Orthopaedic Translation

journal homepage: www.journals.elsevier.com/journal-of-orthopaedic-translation

ORIGINAL ARTICLE

One strike loading organ culture model to investigate the post-traumatic disc degenerative condition

Zhiyu Zhou [a,b,c,1], Shangbin Cui [b,c,1], Jie Du [b], R. Geoff Richards [b,c], Mauro Alini [b], Sibylle Grad [b], Zhen Li [b,*]

[a] The Seventh Affiliated Hospital of Sun Yat-sen University, Shenzhen, China
[b] AO Research Institute Davos, Davos, Switzerland
[c] Guangdong Provincial Key Laboratory of Orthopedics and Traumatology, The First Affiliated Hospital of Sun Yat-sen University, Guangzhou, China

ARTICLE INFO

Keywords:
Degeneration
Extracellular matrix
Intervertebral disc
Mechanical injury
One strike loading
Post-traumatic

SUMMARY

Background: Acute trauma on intervertebral discs (IVDs) is thought to be one of the risk factors for IVD degeneration. The pathophysiology of IVD degeneration induced by single high impact mechanical injury is not very well understood. The aim of this study was using a post-traumatic IVD model in a whole organ culture system to analyze the biological and biomechanical consequences of the single high-impact loading event on the cultured IVDs.

Methods: Isolated healthy bovine IVDs were loaded with a physiological loading protocol in the control group or with injurious loading (compression at 50% of IVD height) in the one strike loading (OSL) group. After another 1 day (short term) or 8 days (long term) of whole organ culture within a bioreactor, the samples were collected to analyze the cell viability, histological morphology and gene expression. The conditioned medium was collected daily to analyze the release of glycosaminoglycan (GAG) and nitric oxide (NO).

Results: The OSL IVD injury group showed signs of early degeneration including reduction of dynamic compressive stiffness, annulus fibrosus (AF) fissures and extracellular matrix degradation. Compared to the control group, the OSL model group showed more severe cell death ($P < 0.01$) and higher GAG release in the culture medium ($P < 0.05$). The MMP and ADAMTS families were up-regulated in both nucleus pulposus (NP) and AF tissues from the OSL model group ($P < 0.05$). The OSL injury model induced a traumatic degenerative cascade in the whole organ cultured IVD.

Conclusions: The present study shows a single hyperphysiological mechanical compression applied to healthy bovine IVDs caused significant drop of cell viability, altered the mRNA expression in the IVD, and increased ECM degradation. The OSL IVD model could provide new insights into the mechanism of mechanical injury induced early IVD degeneration.

The translational potential of this article: This model has a high potential for investigation of the degeneration mechanism in post-traumatic IVD disease, identification of novel biomarkers and therapeutic targets, as well as screening of treatment therapies.

Introduction

Low back pain is often related to intervertebral disc (IVD) degeneration. While painful IVD degeneration is not a lethal disease, it has been recognized as a major social burden with a high socioeconomic impact, with many people not being able to return to work. Low back pain has been reported as the leading cause of disability worldwide, with a total cost of more than $100 billion annually in the United States alone [1,2]. Prevention and therapeutic intervention are hampered because the veritable cause of low back pain often remains unclear. Although a correlation with IVD degeneration has been documented [3], the etiology of IVD degeneration as the cause of low back pain is still obscure. The current consensus is that IVD degeneration is a multi-factorial disease [4–6].

The function of IVDs is to provide load-bearing and range of motion to the trunk, neck and head. Traditional concepts on the function of the disc

* Corresponding author. AO Research Institute Davos, Clavadelerstrasse 8, 7270 Davos Platz, Switzerland.
E-mail address: zhen.li@aofoundation.org (Z. Li).
[1] The first two authors contributed equally to the article.

https://doi.org/10.1016/j.jot.2020.08.003
Received 15 April 2020; Received in revised form 1 July 2020; Accepted 9 August 2020
Available online 20 October 2020

relate to specific extracellular matrix (ECM) proteins that assemble and interact to form the 3 distinct structures. While one can describe the nucleus pulposus (NP), annulus fibrosus (AF) and cartilage endplate (EP) separately with distinct functions, the homeostasis of the IVD as a unit must have optimal function from all 3 structures. The impairment of one or more of these structures can lead to IVD degeneration [7].

The healthy NP is a gel-like [8,9], highly hydrated tissue rich in proteoglycans. The NP generates an intradiscal pressure which resists the compression from the adjacent vertebrae and the tension from the surrounding AF, and distributes pressure evenly over the two adjacent endplates. A degenerated NP is an unorganized fibrous tissue which has largely lost its capacity to bind water under compression. Therefore, the pressure in the NP is diminished and disc height is lost [10]. Narrowing of the disc space has also been commonly observed after fractures of the thoracolumbar spine, which is associated with progressive kyphosis and pain in patients treated conservatively or with recurrent kyphosis after posterior reduction and fixation [11,12].

The healthy AF is a highly organized fibrous structure. It consists of more than 20 concentric lamellae of alternating oblique collagen fibers interspersed with proteoglycans. The collagen fibers resist a high intradiscal pressure from two sources: direct radial pressure from the NP, and cranial-caudal stretch from the two adjacent endplates. Due to the loss of intradiscal pressure, the AF of a degenerated IVD deforms by in- and outward bulging and buckling, and shows progressive increase of structural defects such as rim lesions, delamination and radial fissures [13,14].

Animal models and organ culture models are important preclinical tools for biomedical research [15,16]. Ideally, the most appropriate preclinical model for a specific disease is to artificially develop a condition that replicates the human condition. Due to the complicated etiology and pathogenesis of disc degeneration, developing a suitable preclinical model is challenging because it should share features that are similar to disc degeneration in human and it should be reliable, reproducible as well as cost and labor efficient. Currently, there are 4 major categories of preclinical IVD degeneration models: (1) genetic model, (2) mechanical loading, (3) direct structural disruption including annulus/nucleus injury, chemical digestion, and endplate injury, and (4) radicular pain [17–19], which mimic the triggers in various disease phenotypes of IVD degeneration. The current study focused on the simulation of a post-traumatic IVD degeneration phenotype [17,20].

It has been shown that disc degeneration may originate from biomechanical wear and tear [4,21–23]. Notably, the risk of disc degeneration is increased in manual laborers such as carpenters and drivers of machinery [24]. Excessive mechanical loading or acute trauma to IVDs is thought to contribute to the degeneration and pain [15,25–27]. Ghanem et al. reported that pathological signal changes of the IVD on magnetic resonance imaging (MRI) can be observed after spine trauma [28]. The exact mechanisms by which acute mechanical injury initiates and promotes degeneration is still unclear.

In recent years, bovine IVD organ culture models have gained popularity since the dimensions and biological composition of bovine IVDs is relatively equivalent to human discs [20]. Investigating the degeneration mechanism and therapeutic treatment in whole IVD explants in combination with a specific loading regime may represent a way to bridge the gap between in-vitro and in-vivo tests [29,30].

The aim of this study was using a post-traumatic IVD model in a whole organ culture system to analyze the biological and biomechanical consequences of the single high-impact loading event on the cultured IVDs. The diurnal disc height loss of human lower lumbar discs had been reported to reach 11.1% [31]. Based on that, our previous study defined a physiological loading protocol for bovine caudal IVDs cultured within bioreactors [32], which caused a 10% disc height loss after loading and served as the physiological control group in the current study. To mimic an acute traumatic injury, the model group was subjected to one strike compressive loading at a 50% strain of the disc height. After physiological loading for another 1 or 8 days, the cell viability, matrix organization, gene expression and mechanical properties of IVDs were analyzed (Fig. 1).

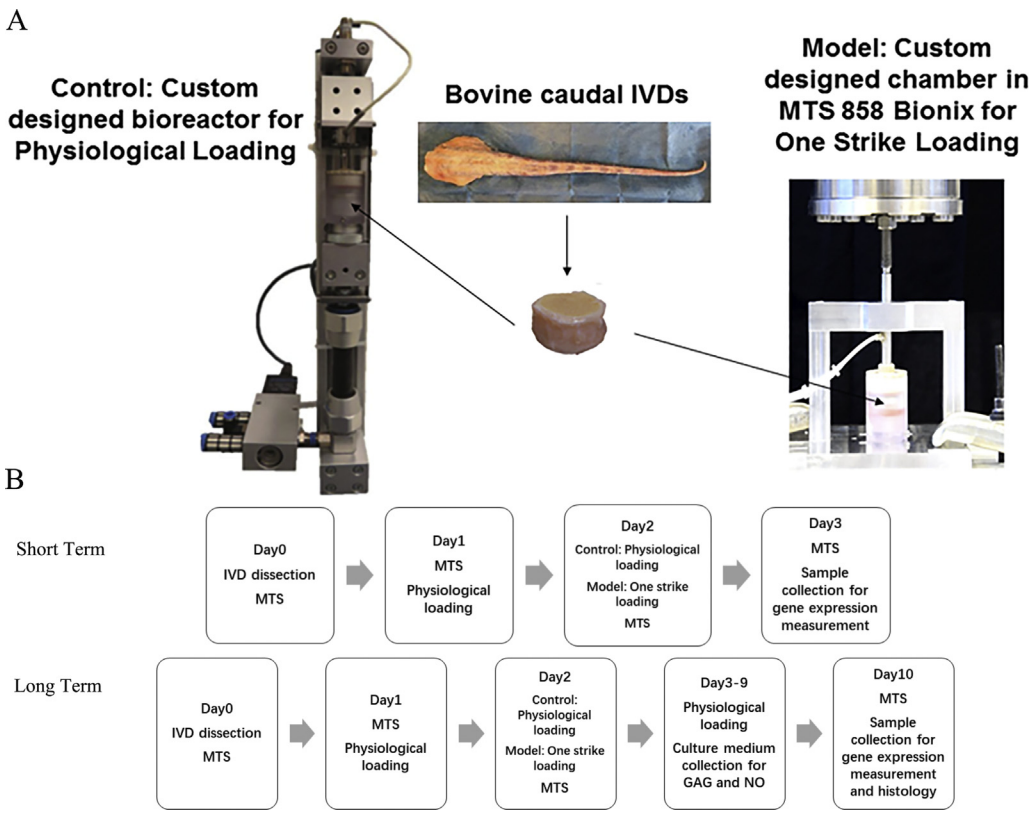

Fig. 1. (A) The bioreactor for physiological loading, and MTS machine with custom designed chamber for one strike loading on bovine IVDs. **(B)** The experiment design flow chart of short term and long term studies.

Materials and methods

Dissection and culture of bovine intervertebral discs with endplates

Caudal bovine IVDs were obtained from 4 to 10 months animals as previously described [22]. Briefly, after removal of the soft tissues, IVDs comprising endplates were harvested using a band-saw. The endplates (1–2 mm thickness) were rinsed with Ringer solution using the Pulsavac jet-lavage system (Zimmer, Warsaw, Indiana, USA). The discs were further incubated in 1000 units/mL penicillin, 1000 μg/mL streptomycin in phosphate buffered saline (PBS) solution for 10 min. The cleaned discs were transferred to 6 well-plates and kept in an incubator at 37°C, 85% humidity and 5% CO_2 until the next day. The culture medium was composed of Dulbecco's modified Eagle medium (DMEM) containing 4.5 g/L glucose and supplied with 2% foetal calf serum, 1% ITS + Premix (Discovery Labware, Inc., Bedford, USA), 50 μg/mL ascorbate-2-phosphate (Sigma–Aldrich, St. Louis, USA), non essential amino acids, 100 units/mL penicillin, 100 μg/mL streptomycin (all except for mentioned, Gibco, Basel, Switzerland) and 0.1% Primocin (Invitrogen, San Diego, CA, USA). Discs (mean IVD height 9.47 ± 1.27 mm, mean IVD diameter 15.96 ± 1.75 mm) were systematically assigned to one of three groups: One Strike Loading model, Physiological loading control, Day0 group.

Loading protocol

The physiological loading was performed with our custom designed bioreactor at 0.02–0.2 MPa, 0.2 Hz, 2 h per day. The bioreactor was maintained in an incubator at 37°C, 85% humidity and 5% CO_2. One strike loading was performed using a Mini Bionix 858 MTS machine and the custom designed chamber. In a preliminary experiment, one strike loading at different strains of 10%, 20%, 30%, 40%, and 50% were applied on IVDs. Gene expression results showed that the 50% reduction of disc height induced most pronounced changes in the degeneration process, as indicated by higher expression of MMP3, ADAMTS4, ADAMTS5 in the NP tissue and MMP13 in the AF tissue (Supplementary Fig. 1). Therefore, one strike loading at 50% strain was chosen for the following study. In the main study, IVDs were held under a mild load of 10 N (~0.1 MPa) for 3 min to make sure that the load cell was in contact with the IVDs, followed by compression to 50% of disc height in 1 s. The average peak stress achieved in one strike loading (OSL) model group was 35.461 ± 8.274 MPa. After loading, the IVDs were cultured in 6-well plates for overnight free swelling recovery. The medium of the IVD samples was changed twice a day, after free swelling and after loading. After physiological loading or one strike loading on day 2, the IVDs were cultured with physiological loading for another 1 or 8 days (Fig. 1).

Measurement of disc height changes

The mean disc height (including endplates) was measured with a caliper at different time points [33]: on day 0 immediately after dissection; on day 1 to day 10 after overnight free swelling culture and after loading. Each disc was measured at 2 positions for disc height and the average value was used to calculate percentage of disc height change and normalized to the initial dimension after dissection.

Measurement of dynamic compressive stiffness

The dynamic compressive stiffness was measured for each disc at different time points: on day 0 after dissection, on day 1 after free swelling culture overnight (Day1 swelling), on day 2 after different loading regime (Day2 after model), and on day 3 after overnight free swelling recovery (Day3 model swelling). Measurement was performed using a custom-made chamber and MTS Acuman [34]. Discs were pre-loaded with 10% strain (based on disc height measured before stiffness evaluation) for 3 min, and then loaded with 10 cycles of sinusoidal compression at 5–15% of strain (based on disc height measured before stiffness evaluation). Dynamic stress was calculated as (Fmax–Fmin)/S, where Fmax and Fmin are the maximum and minimum forces reached during one cycle and S is the surface area of the disc (as measured at dissection). Dynamic compressive stiffness was calculated for each loading cycle as dynamic stress divided by the applied strain. The average value of 10 cycles was taken for each disc at each time point. The stiffness was measured on each disc on day 0 after dissection and used as baseline for normalization.

Histology

After 10 days of culture, IVDs were snap-frozen and embedded in cryo-embedding compound (Tissue-Tek, O.C.T.TM, Sismex, Horgen, Switzerland). Transverse sections of IVDs were made at a thickness of 10 μm. Sections were stained with 0.1% Safranin-O (Chroma Gesellschaft, Munster, Germany) and 0.02% Fast Green (Fluka, Seelze, Germany) to reveal proteoglycan and collagen deposition respectively and counter-stained with Weigert's Haematoxylin to reveal cell distribution. The sections were imaged in transmitted light under an upright optical microscope (Axioplan 2, Zeiss, Germany). The acquisition time was kept constant for all samples.

A semi-quantitative scoring scheme adapted from Shu et al. [35] was used to evaluate the Safranin O/Fast Green staining. IVD structure/cleft characteristics were summed up to assess the degree of IVD degeneration (Table 1).

Cell viability

Cell viability was assessed using the lactate dehydrogenase (LDH) method, by staining with LDH and ethidium homodimer [29]. Six random images (623 × 623 μm) were taken from different areas in three different zones: the NP, the inner AF and the outer AF in each section (n = 8). The numbers of alive and dead cells per image area were counted using ImageJ. Cells stained blue (LDH) or blue/red (ethidium homodimer) were counted as alive cells. Cells stained red only were counted as dead cells.

Analysis of gene expression

Disc tissue was collected on day 3 or day 10 for gene expression measurement. Cartilaginous endplates of each IVD were removed, and NP and AF tissues were harvested using a biopsy punch and a scalpel blade. Approximately 150 mg of each NP and AF tissue was used for RNA extraction.

Table 1
Histological score grading criteria.

Grade	Histological degeneration
IVD structure. Histology cross section clefts characteristics	
0	normal IVD structure with well defined annular lamellae, central NP
1	clefts evidence in IAF, normal NP morphology
2	clefts evident in IAF, mild clefts in OAF, inverted IAF lamellae with anomalous distortions
3	Bifurcation/propagation of clefts from IAF into NP margins, mild delamination, or concentric tears between lamellae in IAF
4	Propagation of cleft into NP, with disruption in normal NP structure, distortion of annular lamellae into atypical arrangements-severe delamination, separation of translamellar cross bridges
Formation of clefts	
0	No clefts in AF
1	Small clefts area in AF (width of cleft in the range of 90–180 μm)
2	Moderate clefts area in AF (the number of clefts ≤ 3, width> 180 μm)
3	Large clefts area in AF (the number of clefts >3, width>180 μm)
Clefts direction	
0	clefts were parallel to the AF lamellae
2	Clefts were perpendicular to the AF lamellae.

AF = annulus fibrosus; IAF = inner AF; OAF = outer AF; NP = nucleus pulposus

For RNA extraction, tissue samples were digested with 2 mg/mL pronase for 1 h at 37°C, flash frozen, pulverized in liquid nitrogen, and homogenized using a TissueLyser (Qiagen, Venlo, Netherlands) [36]. Total RNA was extracted with TRI Reagent (Molecular Research Center), and reverse transcription was performed with SuperScript VILO cDNA Synthesis Kit (Life Technologies, Carlsbad, CA). Quantitative real-time polymerase chain reaction was performed using the Quant Studio 6 instrument (Life Technologies).

The sequences of custom designed bovine primers and TaqMan™ probes are shown in Table 2. For amplification of ribosomal protein large P0 (RPLP0, Bt03218086_m1), CD146 (Bt03258894_m1), CXCL5 (Bt03259300_m1), CXCL12 (Bt03276322_m1), and NRN1 (Bt03235564_m1), gene expression assays from Applied Biosystems (Life Technologies) were used. Comparative Ct method was performed for relative quantification of target mRNA with RPLP0 as endogenous control [29].

Table 2
Oligonucleotide primers and probes (bovine) used for quantitative real-time polymerase chain reaction.

Gene	Primer/Probe Type	Sequence
MMP1	Primer forward (5′-3′)	5′-TTC AGC TTT CTC AGG ACG ACA TT-3′
	Primer reverse (5′-3′)	5′-CGA CTG GCT GAG TGG GAT TT-3′
	Probe (5′FAM/3′TAMRA)	5′-TCC AGG CCA TCT ACG GAC CTT CCC-3′
MMP3	Primer forward (5′-3′)	5′-GGC TGC AAG GGA CAA GGA A-3′
	Primer reverse (5′-3′)	5′-CAA ACT GTT TCG TAT CCT TTG CAA-3′
	Probe (5′FAM/3′TAMRA)	5′-CAC CAT GGA GCT TGT TCA GCA ATA TCT AGA AAA C-3′
MMP13	Primer forward (5′-3′)	5′-CCA TCT ACA CCT ACA CTG GCA AAA G-3′
	Primer reverse (5′-3′)	5′-GTC TGG CGT TTT GGG ATG TT-3′
	Probe (5′FAM/3′TAMRA)	5′-TCT CTC TAT GGT CCA GGA GAT GAA GAC CCC-3′
ADAMTS4	Primer forward (5′-3′)	5′-CCC CAT GTG CAA CGT CAA G-3′
	Primer reverse (5′-3′)	5′-AGT CTC CAC AAA TCT GCT CAG TGA-3′
	Probe (5′FAM/3′TAMRA)	5′-AGC CCC CGA AGG GCT AAG CGC-3′
ADAMTS5	Primer forward (5′-3′)	5′-GAT GGT CAC GGT AAC TGT TTG CT-3′
	Primer reverse (5′-3′)	5′-GCC GGG ACA CAC CGA GTA C-3′
	Probe (5′FAM/3′TAMRA)	5′-AGG CCA GAC CTA CGA TGC CAG CC-3′
IL-1b	Primer forward (5′-3′)	5′-TTA CTA CAG TGA CGA GAA TGA GCT GTT-3′
	Primer reverse (5′-3′)	5′-GGT CCA GGT GTT GGA TGC A-3′
	Probe (5′FAM/3′TAMRA)	5′-CTC TTC ATC TGT TTA GGG TCA TCA GCC TCA A-3′
IL-6	Primer forward (5′-3′)	5′-TTC CAA AAA TGG AGG AAA AGG A-3′
	Primer reverse (5′-3′)	5′-TCC AGA AGA CCA GCA GTG GTT-3′
	Probe (5′FAM/3′TAMRA)	5′-CTT CCA ATC TGG GTT CAA TCA GGC GATT-3′
TNF-α	Primer forward (5′-3′)	5′-CCT CTT CTC AAG CCT CAA GTA ACA A-3′
	Primer reverse (5′-3′)	5′-GAG CTG CCC CGG AGA GTT-3′
	Probe (5′FAM/3′TAMRA)	5′-ATG TCG GCT ACA ACG TGG GCT ACC G-3′
ACAN	Primer forward (5′-3′)	5′-CCA ACG AAA CCT ATG ACG TGT ACT-3′
	Primer reverse (5′-3′)	5′-GCA CTC GTT GGC TGC CTC-3′
	Probe (5′FAM/3′TAMRA)	5′-ATG TTG CAT AGA AGA CCT CGC CCT CCA T-3′
COL2	Primer forward (5′-3′)	5′-AAG AAA CAC ATC TGG TTT GGA GAA A-3′
	Primer reverse (5′-3′)	5′-TGG GAG CCA GGT TGT CAT C-3′
	Probe (5′FAM/3′TAMRA)	5′-CAA CGG TGG CTT CCA CTT CAG CTA TGG-3′

Analysis of conditioned medium

Conditioned medium was collected for analysis of released matrix components and mediators. The GAG content in the conditioned medium was determined using the DMMB method [37]. Levels of nitric oxide (NO) in the conditioned medium of IVDs were determined as the concentration of its stable oxidation product, nitrite (NO^{2-}), using the Griess Reagent Kit (Promega, Madison, USA [32]).

Statistical analysis

Statistical analysis was performed using GraphPad Prism 7 software (GraphPad Software, Inc., La Jolla, CA, USA). D'Agostino-Pearson omnibus normality test was used to define whether the data were normally distributed. For data that were normally distributed, unpaired *t*-test was used to determine differences between two groups; one-way ANOVA was used to determine differences between three or more groups. For data that were not normally distributed, Mann–Whitney U test was used to determine differences between two groups; Kruskal Wallis test was used to determine differences between three or more groups. $p < 0.05$ was considered statistically significant.

Results

Disc height change and dynamic compressive stiffness

After first day free swelling, the disc height changes of control group and model group did not show any significant difference. However, on day 2 after loading, the disc height loss of the model group was greater than the control group. Furthermore, the disc height recovery after free swelling was significantly reduced in the model compared to the control group on day 3. After longer term culture, the disc height of the model group still did not fully recover, as indicated by significantly lower disc height compared with the control group on day 10 (Fig. 2A).

At each time point, dynamic compressive stiffness was normalized to the original value of the respective disc on day 0 after dissection. Compared with the physiological loading control group, one strike loading reduced the stiffness of IVDs after model induction on day 2, which did not recover after free swelling culture on day 3 (Fig. 2B, $P < 0.05$).

Cell viability and disc morphology

The lactate dehydrogenase (LDH)/Ethidium homodimer staining images of each group are shown in Fig. 3. One strike loading caused significant IVD cell death. The number of alive cells, dead cells and the cell viability are shown in Fig. 4. Physiologically loaded IVDs on day 10 showed significantly lower alive cell numbers compared with IVDs dissected on day 0 in the NP and inner AF regions (Fig. 4 A1 and A2, $P < 0.05$). While the one strike model group showed markedly lower alive cell numbers compared with Day 0 group in all the three disc regions (Fig. 4A, $P < 0.05$). Compared with the physiological group on day 10, the one strike model group also showed significantly lower alive cell numbers in the inner and outer AF regions (Fig. 4 A2 and A3, $P < 0.05$). The numbers of dead cells in NP, inner AF and outer AF are shown in Fig. 4B. In the outer AF region, the one strike model group had significantly higher dead cell numbers compared with the other two groups (Fig. 4 B3, $P < 0.05$). The cell viability in the NP region was significantly reduced in the physiological group on day 10 compared with day0

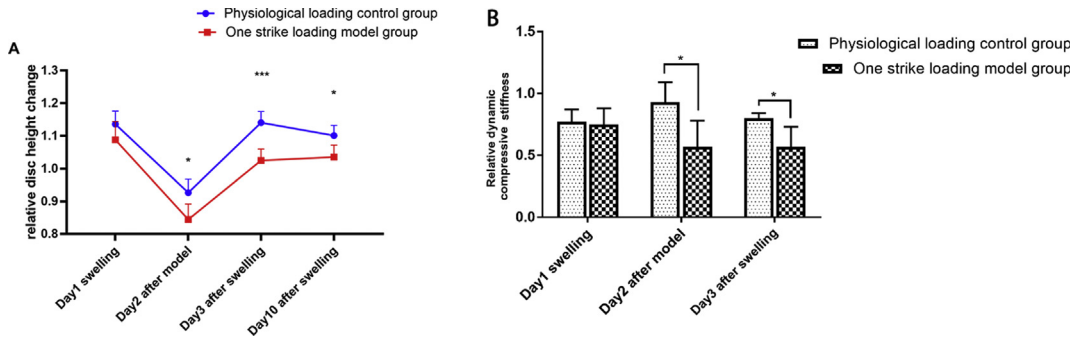

Fig. 2. Disc height change **(A)** and Dynamic compressive stiffness **(B)** of the IVDs measured on day 0 after dissection, on day 1 after overnight free swelling (Day1 swelling), on day 2 after loading (Day2 after model), on day 3 and day 10 after overnight free swelling recovery (Day3/Day10 after swelling). Data were normalized to original height and dynamic compressive stiffness of each disc on day 0 after dissection, Mean +SD, n = 5, *p < 0.05, ***P < 0.001.

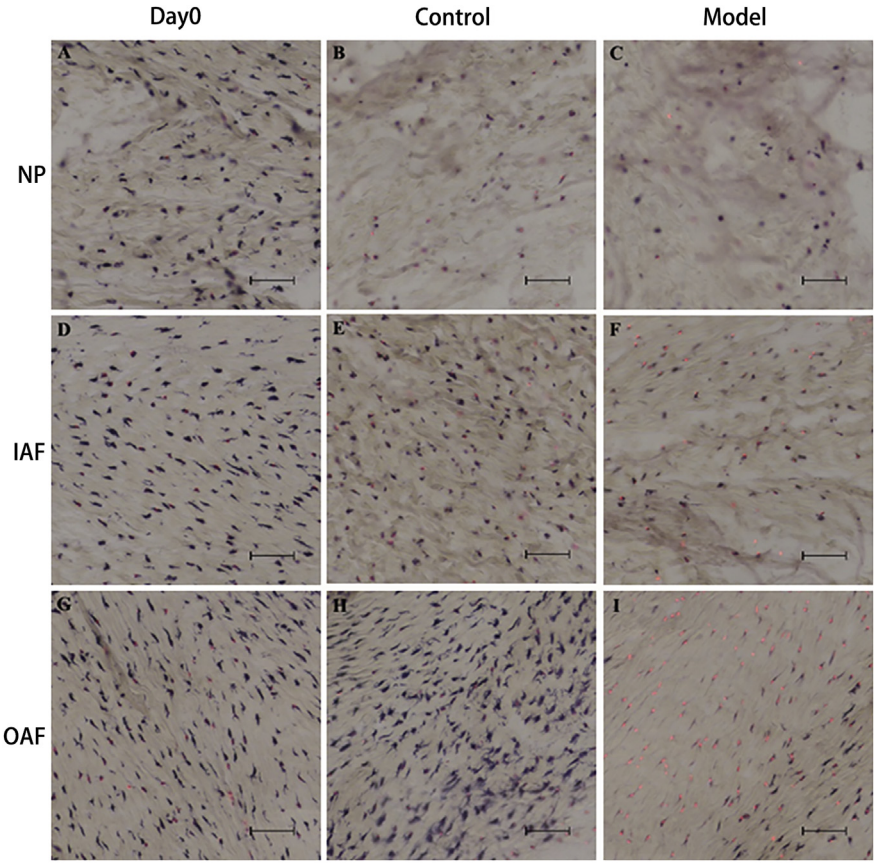

Fig. 3. Representative LDH/Ethidium homodimer staining images of IVDs collected on day 0 after dissection (Day 0, **A, D, G**), and on day 10 after physiological loading (Control, **B, E, H**) or one strike loading (Model, **C, F, I**). Cell viability was assessed using LDH/Ethidium homodimer staining (blue and blue/red = alive cell; red only = dead cell). Figures A, B, C represent NP tissue. Figures D, E, F represent inner AF (IAF) tissue. Figures G, H, I represent outer AF (OAF) tissue. Scale bar: 100 μm.

(Fig. 4C1, P < 0.05). One strike loading did not further affect the cell viability in the NP region. In the inner and outer AF regions, the physiological loading group on day 10 showed comparable cell viability to day 0, while one strike loading significantly reduced the cell viability compared to the other two groups (Fig. 4C2 and C3, P < 0.05).

Safranin O/Fast Green staining images of the cross sections from discs on day 10 are shown in Fig. 5. A histological modified scoring standard was used based on literatures [26,35] (Table 1). Different cleft patterns were found in the AF tissue of IVDs from control and one strike model groups. In the control group, mild clefts were found in IAF and OAF. Most of the clefts were without anomalous distortions. In one strike model group, bifurcation/propagation of clefts from IAF into NP margins, and mild delamination were found in most samples. Some samples showed propagation of clefts into NP and severe delamination. In the control group, only small cleft areas were found in the AF. However, in the one strike group, moderate and large cleft areas were found in the AF. As for the clefts' direction, there were more clefts both perpendicular and parallel to the AF lamellae in the one strike model group. The Day0 group had significantly lower scores than the physiological loading control group (Fig. 5, P < 0.05). Moreover, the physiological loading control group had significantly lower scores than the one strike loading model group (Fig. 5, P < 0.05).

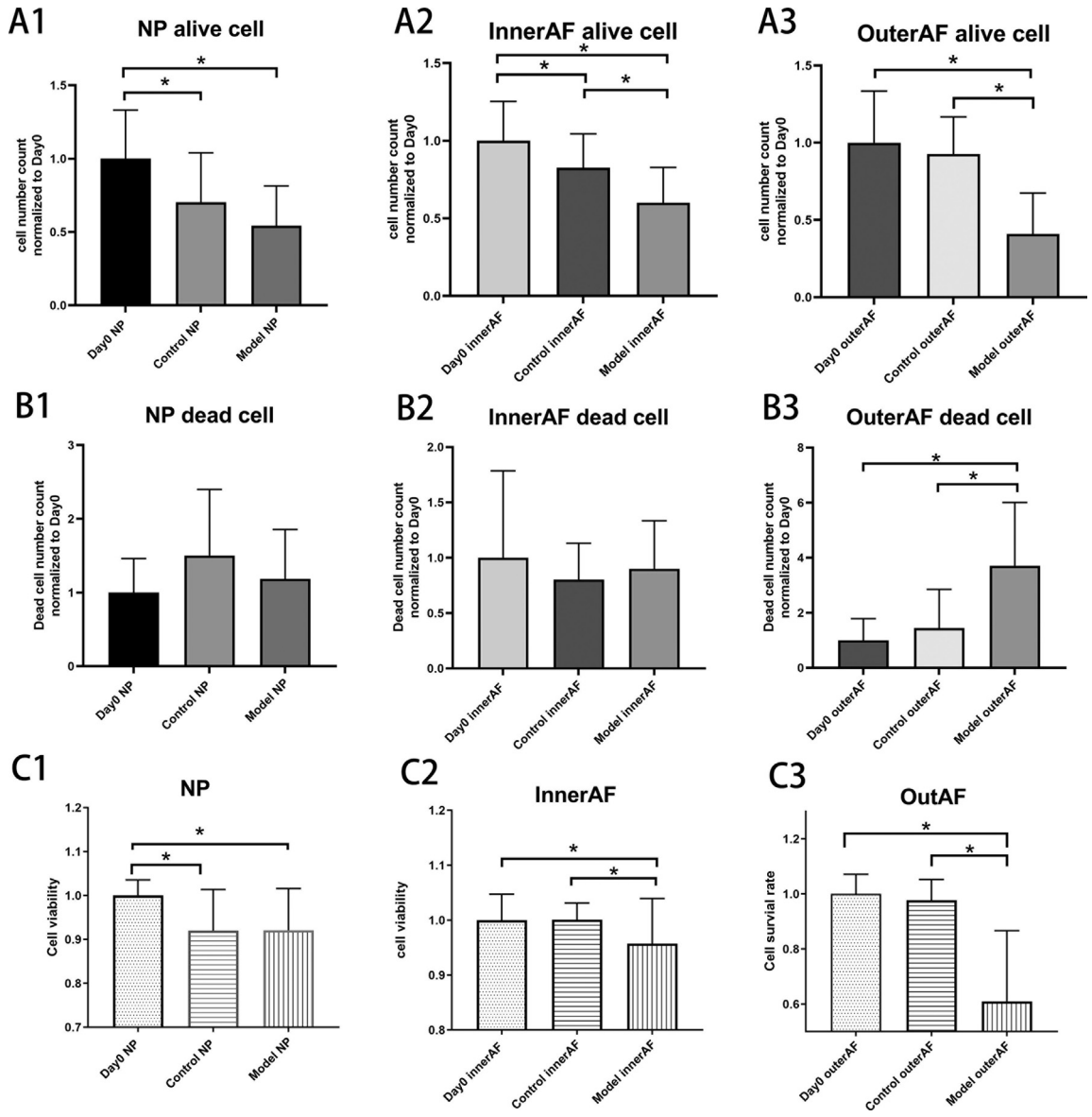

Fig. 4. The numbers of alive cells, dead cells (per 40,000 μm^2) and cell viability from different groups. **A1, B1, C1** represent NP region; **A2, B2, C2** represent inner AF (IAF) region; **A3, B3, C3** represent outer AF (OAF) region. Mean + SD, *p < 0.05, the data were normalized to day0 group (n = 8).

Release of nitric oxide (NO) and glycosaminoglycans (GAG) in IVD conditioned medium

Conditioned medium was collected daily during the free swelling period and loading period for the measurement of released molecules. The NO and GAG secreted into culture media were measured and normalized to the disc volume. The NO released from model and control groups was not statistically different (Fig. 6A). A significantly higher GAG release from the model group was observed compared to the control group, starting from day 4 after overnight free swelling until the end of the experiment (Fig. 6B, $p < 0.05$).

One strike loading alters the mRNA expression in IVD tissue

The model group and control group IVD samples were collected for gene expression measurement on day 3 (short term, Fig. 6C and D) or on day 10 (long term, Fig. 6 E and F). The expressions of various anabolic, catabolic and pro-inflammatory genes in NP and AF tissue were measured using real time RT-PCR. Compared to the control group, in the short term experiment, the gene expressions of MMP1, MMP3, ADAMTS4, ADAMTS5, CXCL5, and IL-6 were up-regulated in NP but not in AF of the one strike loading model group (Fig. 6C and D, $p < 0.05$). In the long term experiment, the gene expressions of MMP1, MMP13 and ADAMTS5 in AF but not in NP of the one strike loading model group were up-regulated (Fig. 6 E and F, $p < 0.05$).

Discussion

The development of appropriate preclinical models of IVD degeneration is necessary to gain insight into the pathophysiology and to develop and test potential therapies. A range of animal and organ models and mechanisms of replicating the process of degeneration have been investigated and utilized. Bovine is among the fewer animal species which lose the notochordal cells rapidly from NP following birth, and the numbers decrease rapidly with aging. Histology images of a 6 months old bovine caudal disc showed absence of cells with notochordal morphology in the nucleus pulposus tissue, which is like in adolescent human discs [29,38]. Moreover, the characteristic dimension of bovine disc height which determines the transport rate of nutrients and metabolites and ultimately has a profound effect on the density of live cells in the IVD is quite similar to

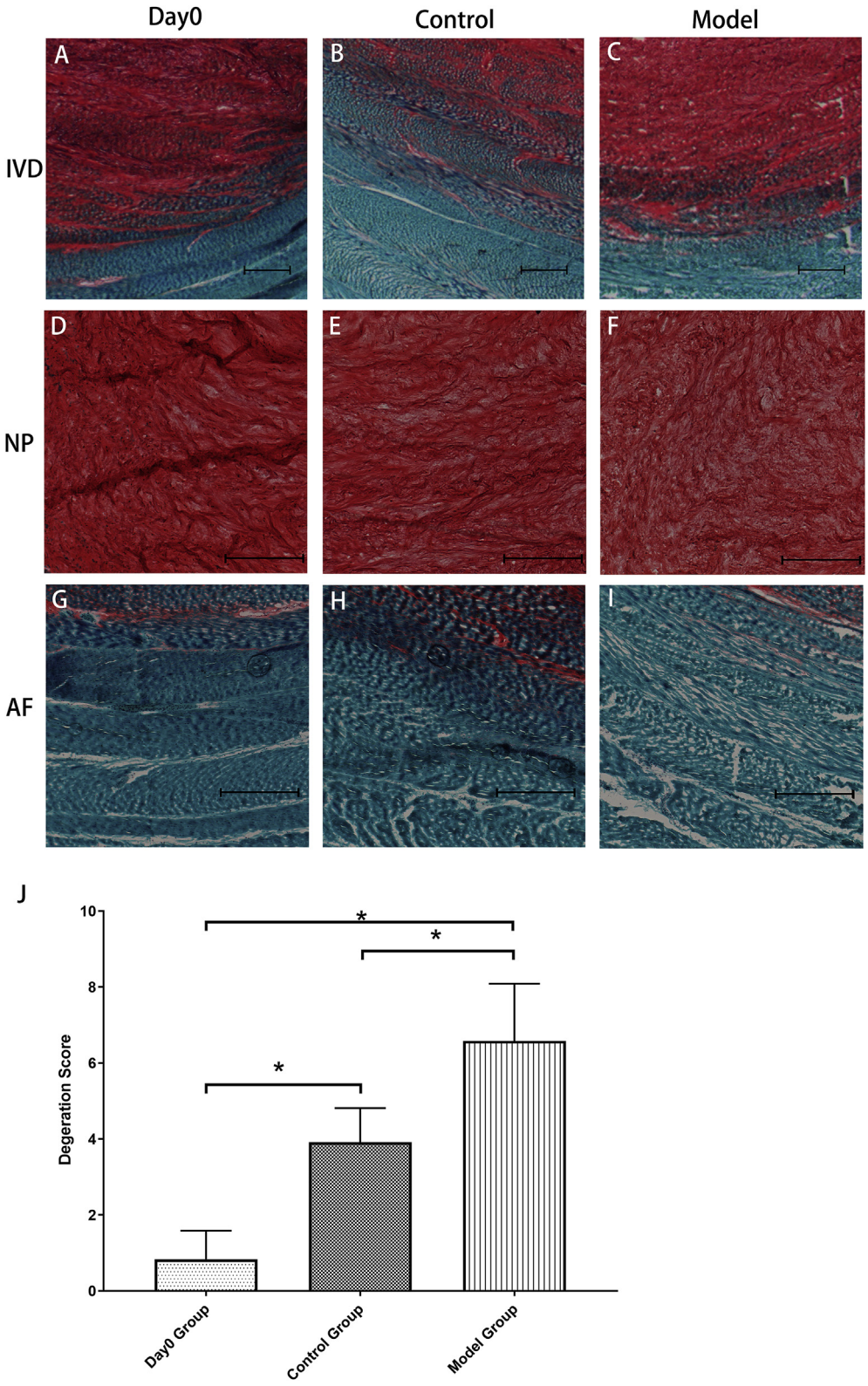

Fig. 5. Representative Safranin O/Fast green staining images of cross histological sections from IVDs on day 0 after dissection (Day 0, **A, D, G**), on day 10 after physiological loading (Control, **B, E, H**), and on day 10 after one strike loading (Model, **C, F, I**). Scale bar: 500 μm. (J) Histological scoring values based on Safranin O/Fast green staining (n = 3).

that of human [39]. For the reasons above, bovine IVDs were selected in this study to investigate the cell response after high impact loading.

Here, we demonstrate that acute mechanical injury initiates events associated with disc degeneration in an ex vivo bioreactor cultured bovine whole-organ model. Loading schemes of non-injurious loading of 0.02–0.2 MPa, 0.2 Hz and injurious loading at a high speed (50% strain per second) were applied, simulating normal physiological and acute hyperphysiological compression respectively. The one strike loading

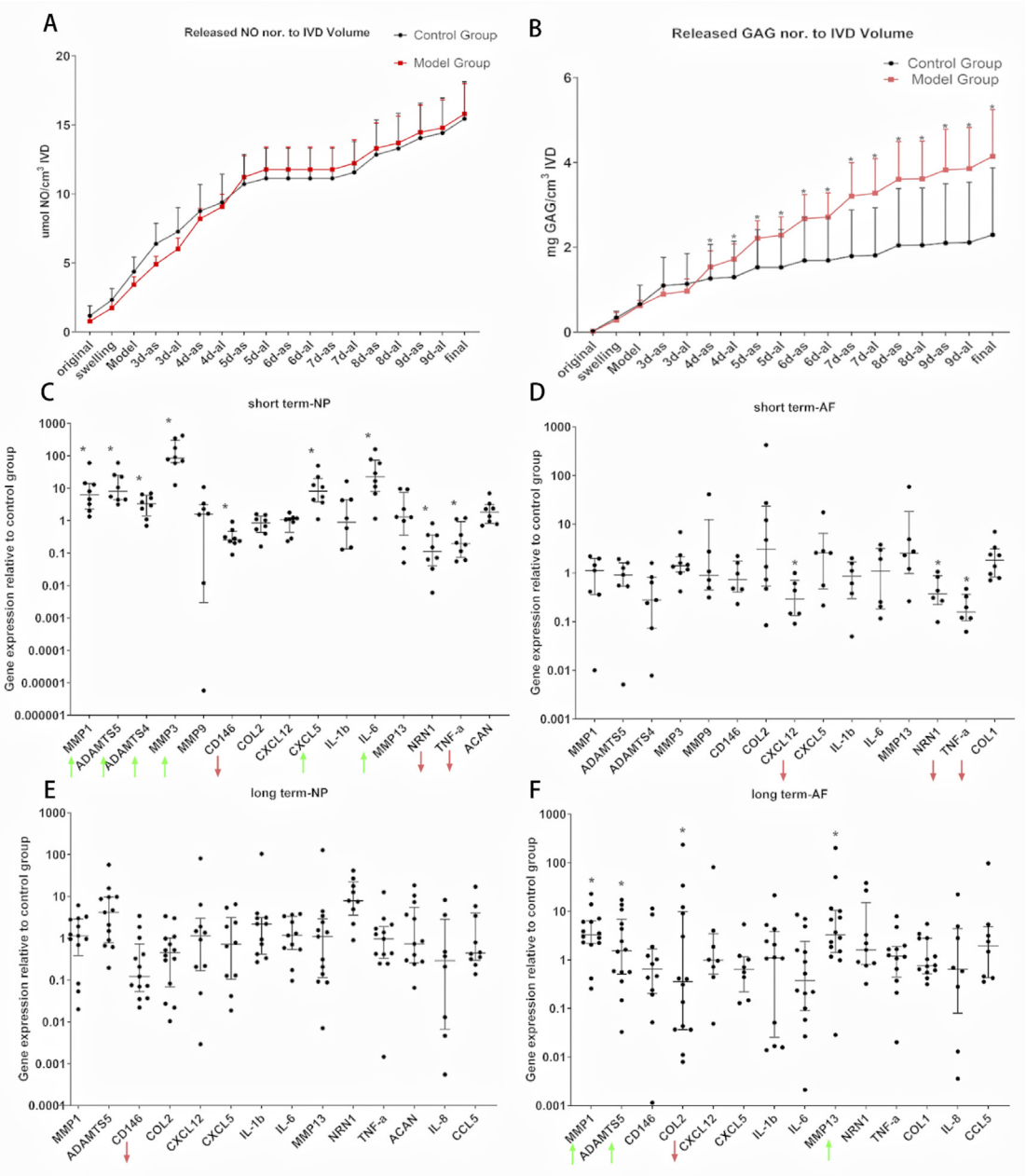

Fig. 6. Accumulative NO **(A)** and GAG **(B)** release in conditioned media of IVDs cultured with physiological loading (Control Group) or one strike loading (Model Group) during culture. Mean + SD, n = 3, as = after free swelling overnight recovery, al = after loading, NO = nitric oxide, GAG = glycosaminoglycan. Gene expression in NP **(C, E)** and AF **(D, F)** tissue of Model group normalized to Control group as 1, on day 3 in short term experiment (C, D, n = 8), or on day 10 in long term experiment (E, F, n = 14). *p < 0.05; ↑ indicates the gene expression was significantly upregulated in Model group compared to Control group, ↓ indicates the gene expression was significantly downregulated in Model group compared to control group.

pattern is more likely to simulate the clinical cases of a high altitude falling accident. In our study, acute mechanical injury caused annulus clefts, drop of cell viability, upregulated expression of catabolic enzymes, and significant loss of proteoglycan. The disc height and dynamic compressive stiffness of IVDs in the model group showed a significant drop compared with the control group and neither returned to their original level at short nor at long term culture on day 3 and day 10. In the one strike group, the IVD was impacted by a high loading which damaged the microstructure of the IVD, as shown by more clefts in the AF tissue. The integrity of the IVD was shattered and therefore the dynamic compressive stiffness decreased after one strike loading due to tissue softening. These results indicate that the one strike loading caused permanent damage to the disc structure which lost the ability to recover.

Some researchers hypothesize that disc degeneration originates from biomechanical wear and tear [31]. This has long been thought to be a major cause of IVD degeneration, mainly because low back pain and degeneration occur more frequently in the working population, including manual labor workers, machine drivers, soldier carrying loads, but also in elite athletes [40]. A strong link between high loading on the low back and IVD degeneration has been reported [20]. Haschtmann et al. established a rabbit disc/endplate trauma culture model to reproducibly induce endplate fractures and investigate concurrent disc changes in vitro. Disc trauma resulted in a number of biological changes such as necrotic and up-regulation of caspase 3 gene which are involved in apoptotic pathway accompanied by the induction of collagenases such as MMP1 and MMP13 [41].

Dudli et al. used rabbit spinal segments to establish an in-vitro burst fracture model that more closely mimics the in-vivo situation. Burst fractures were induced by using a dropped-weight device and all the specimens were dynamically loaded daily (~1 MPa nominal pressure, 1 Hz, 2500 cycles). Burst fracture with post-traumatic physiological loading resulted in a 65% loss of GAG/DNA by day 28. Catabolic (MMP-1/-3), pro-apoptotic (TNF-α, fas-ligand), and pro-inflammatory (IL-1/-6, iNOS) gene transcription was substantially up-regulated [42]. Subsequent studies with this model showed that degeneration persisted also in the presence of post-traumatic dynamic loading, pointing towards an immune-regulated response [43]. Other organ culture models used altered biomechanics to induce IVD degeneration. For example, high magnitude cyclic tensile loading of bovine caudal discs permanently disrupted the ECM, and wedge-loading of bovine caudal discs caused a catabolic shift within the ECM reminiscent of degeneration [44–46].

Another study using healthy human cadaveric whole IVD cultures showed that a single, fast mechanical compression of 30% strain was sufficient to cause healthy human IVDs to immediately adapt a degenerate-like phenotype consisting of endplate fracture, significant cell death, proteoglycan cleavage and loss, increased aggrecan fragmentation in the injured tissue and release of pro-inflammatory and neurotrophic factors [18]. However, after mechanical compression, the disc was cultured under free swelling condition. Free-swelling culture mimics the condition of spines and IVDs under low or microgravity and could possibly affect cell viability by changes in osmotic pressure [47,48]. The current study employed IVD organ cutlure under physiological loading after one strike loading injury, which would be essential to maintain the disc homeostasis and the continuous solute exchange, and better reveal the post-traumatic IVD phenotypic changes in the degenerative process.

Traumatic disc injury is an important factor causing IVD cell death, which results in IVD degeneration. A clinical study showed that surgical IVD samples from patients with traumatic injury showed up to 75% cell death [49]. In our one strike loading model, the traumatic impact to healthy bovine IVD caused 14% cell death in NP, 10% cell death in inner AF and 43% cell death in outer AF. This finding is consistent with a previous study from Sitte et al., where the bovine post-trauma group showed disc cell death, mainly necrotic, which was highest in the outer AF and lowest in the NP [49]. We speculate that the more distant from the centre of the disc, the higher the deformation rate the tissue would get. Therefore, the outer AF tissue suffered more shear strain which may have led to more severe cell death.

Proteoglycan fragmentation and loss in water content of human IVDs occur due to normal aging [23]. When these events are accelerated, they become hallmarks of early disc degeneration. Proteoglycan degradation was apparent when adverse loading conditions were applied to the caprine IVD [50]. In our study, MMP1, MMP3, MMP13, ADAMTS4 and ADAMTS5 gene expression were upregulated in short term-NP tissue. Meanwhile, MMP1, MMP13 and ADAMTS5 gene expression were upregulated in long term-AF tissue. The MMP and ADAMTS families gene expression change may be the initiators of disc degeneration processes. Increased GAG release into the culture medium indicated break down of extracellular matrix after one-strike loading. One strike loading did not induce a profound proinflammatory effect, as indicated by unaltered NO release and expression of IL-1β and TNFα.

Our organ culture model with the cartilaginous endplates has the advantage of allowing for diffusion of the nutrients and protein into and out of the discs while maintaining the shape fidelity. After one strike loading, the disc cell viability could be checked in different periods, the conditioned culture media could be analyzed to reveal released matrix degradation products and proinflammatory molecules, and the short-term and long-term response to mechanical injury loading could be evaluated. The present early-onset disc degeneration model will be relevant for investigation of the degeneration mechanism. The concurrent identification of novel diagnostic biomarkers and treatment targets will be essential for the early intervention.

There are some limitations in this study. Firstly, IVD organ culture bioreactors were mainly force-controlled devices which could mimic the natural forces in uni-axial compression only. The cartilaginous endplate model we use in this study lacked several in vivo components of the spine such as ligaments, muscles, zygapophyseal joints, spinous processes and other posterior ligamentous complexes. Lacking complete function unit and complex multidimensional loading, the IVD would show a different deformation comparing to the physiological situation. The peak forces are lower and range of motion greater in caudal IVDs than lumbar IVDs [20,51] so that caution is needed when interpreting results. Secondly, only a set of genes that were already known to be related with IVD degeneration were analyzed. Further study to evaluate the dysregulation in genome and pathways by deep sequencing technique is warranted for more in depth understanding of this model. Moreover, the cartilage endplates were removed for analysis in this study. One strike loading may induce damage on the integrity of the endplate and thus initiate IVD degeneration. Further study will be performed to investigate the mechanism of IVD degeneration induced by integrity failure of endplate after one strike loading. Finally, although the experiment was divided into short-term and long-term comparative analysis, the IVDs were not cultured for an extended time frame, and further follow up of the subsequent degeneration mechanism was not investigated in the current study.

Conclusions

The present study shows a single hyperphysiological mechanical compression applied to healthy bovine IVDs caused significant drop of cell viability, altered the mRNA expression in the IVD, and increased ECM degradation. The one strike loading bovine IVD model could provide new insights into the mechanism of mechanical injury induced early IVD degeneration. This model may be used to further identify biomarkers for diagnosis and therapeutic targets for early intervention in IVD degeneration.

Funding

This research was funded by the National Key R&D Program of China (2017YFC1105000), the AO Foundation, AO Spine International, Switzerland, National Natural Science Foundation of China (51873069, 81772400, 31900583), China Scholarship Council, and Sino-Swiss Science and Technology Cooperation (EG 04-032015).

Role of the funding source

The funders had no role in the design of the study; in the collection, analyses, or interpretation of data; in the writing of the manuscript, or in the decision to publish the results.

Author contributions

Conception and design of study, Z.Z., Z.L., R.G. Richards, and M. Alini; acquisition of data, Z.Z., S.C., J.D., and Z.L.; analysis and/or interpretation of data, Z.Z., S.C., S.G., and Z.L.; drafting the manuscript, S.C., Z.Z., and J.D.; revising the manuscript critically for important intellectual content, R.G.R., M.A., S.G., and Z.L.; supervision, Z.L.; project administration, Z.L.; funding acquisition, R.G.R., M.A., S.G., Z.Z. and Z.L., Approval of the version of the manuscript to be published, S.C., Z.Z., J.D., R.G.R., M.A., S.G., and Z.L.

Conflict of Interest

The authors have no conflicts of interest to disclose in relation to this article.

Appendix A. Supplementary data

Supplementary data to this article can be found online at https://doi.org/10.1016/j.jot.2020.08.003.

References

[1] Wieser S, Horisberger B, Schmidhauser S, Eisenring C, Brugger U, Ruckstuhl A, et al. Cost of low back pain in Switzerland in 2005. Eur J Health Econ 2011;12(5):455–67.
[2] Ricci JA, Stewart WF, Chee E, Leotta C, Foley K, Hochberg MC. Back pain exacerbations and lost productive time costs in United States workers. Spine 2006;31(26):3052–60.
[3] Wang H, Dwyer-Lindgren L, Lofgren KT, Rajaratnam JK, Marcus JR, Levin-Rector A, et al. Age-specific and sex-specific mortality in 187 countries, 1970-2010: a systematic analysis for the Global Burden of Disease Study 2010. Lancet 2012;380(9859):2071–94.
[4] Vergroesen PP, Kingma I, Emanuel KS, Hoogendoorn RJ, Welting TJ, van Royen BJ, et al. Mechanics and biology in intervertebral disc degeneration: a vicious circle. Osteoarthritis Cartilage 2015;23(7):1057–70.
[5] Buckley CT, Hoyland JA, Fujii K, Pandit A, Iatridis JC, Grad S. Critical aspects and challenges for intervertebral disc repair and regeneration-Harnessing advances in tissue engineering. JOR Spine 2018;1(3):e1029.
[6] Gullbrand SE, Smith LJ, Smith HE, Mauck RL. Promise, progress, and problems in whole disc tissue engineering. JOR Spine 2018;1(2):e1015.
[7] Chan WC, Sze KL, Samartzis D, Leung VY, Chan D. Structure and biology of the intervertebral disk in health and disease. Orthop Clin N Am 2011;42(4):447–64. vii.
[8] Ito K, Creemers L. Mechanisms of intervertebral disk degeneration/injury and pain: a review. Global Spine J 2013;3(3):145–52.
[9] Inoue N, Espinoza Orias AA. Biomechanics of intervertebral disk degeneration. Orthop Clin N Am 2011;42(4):487–99. vii.
[10] Antoniou J, Steffen T, Nelson F, Winterbottom N, Hollander AP, Poole RA, et al. The human lumbar intervertebral disc: evidence for changes in the biosynthesis and denaturation of the extracellular matrix with growth, maturation, ageing, and degeneration. J Clin Invest 1996;98(4):996–1003.
[11] Malcolm BW, Bradford DS, Winter RB, Chou SN. Post-traumatic kyphosis. A review of forty-eight surgically treated patients. J Bone Joint Surg Am 1981;63(6):891–9.
[12] Denis F. The three column spine and its significance in the classification of acute thoracolumbar spinal injuries. Spine 1983;8(8):817–31.
[13] Weiler C, Schietzsch M, Kirchner T, Nerlich AG, Boos N, Wuertz K. Age-related changes in human cervical, thoracal and lumbar intervertebral disc exhibit a strong intra-individual correlation. Eur Spine J 2012;21(Suppl 6):S810–8.
[14] Marchand F, Ahmed AM. Investigation of the laminate structure of lumbar disc anulus fibrosus. Spine 1990;15(5):402–10.
[15] Dahia CL, Iatridis JC, Risbud MV. New horizons in spine research: Disc biology, tissue engineering, biomechanics, translational, and clinical research. JOR Spine 2018;1(3):e1032.
[16] Smith LJ, Silverman L, Sakai D, Le Maitre CL, Mauck RL, Malhotra NR, et al. Advancing cell therapies for intervertebral disc regeneration from the lab to the clinic: recommendations of the ORS spine section. JOR Spine 2018;1(4):e1036.
[17] Jin L, Balian G, Li XJ. Animal models for disc degeneration-an update. Histol Histopathol 2018;33(6):543–54.
[18] Alkhatib B, Rosenzweig DH, Krock E, Roughley PJ, Beckman L, Steffen T, et al. Acute mechanical injury of the human intervertebral disc: link to degeneration and pain. Eur Cell Mater 2014;28:98–110. discussion 10-1.
[19] Pfannkuche JJ, Guo W, Cui S, Ma J, Lang G, Peroglio M, et al. Intervertebral disc organ culture for the investigation of disc pathology and regeneration - benefits, limitations, and future directions of bioreactors. Connect Tissue Res 2019:1–18.
[20] Alini M, Eisenstein SM, Ito K, Little C, Kettler AA, Masuda K, et al. Are animal models useful for studying human disc disorders/degeneration? Eur Spine J 2008;17(1):2–19.
[21] Adams MA, Dolan P, McNally DS. The internal mechanical functioning of intervertebral discs and articular cartilage, and its relevance to matrix biology. Matrix Biol 2009;28(7):384–9.
[22] Adams MA, Lama P, Zehra U, Dolan P. Why do some intervertebral discs degenerate, when others (in the same spine) do not? Clin Anat 2015;28(2):195–204.
[23] Adams MA, Freeman BJ, Morrison HP, Nelson IW, Dolan P. Mechanical initiation of intervertebral disc degeneration. Spine 2000;25(13):1625–36.
[24] Luoma K, Riihimaki H, Luukkonen R, Raininko R, Viikari-Juntura E, Lamminen A. Low back pain in relation to lumbar disc degeneration. Spine 2000;25(4):487–92.
[25] Bezci SE, Werbner B, Zhou M, Malollari KG, Dorlhiac G, Carraro C, et al. Radial variation in biochemical composition of the bovine caudal intervertebral disc. JOR Spine 2019;2(3):e1065.
[26] DeLucca JF, Amin D, Peloquin JM, Vresilovic EJ, Costi JJ, Elliott DM. Off-axis response due to mechanical coupling across all six degrees of freedom in the human disc. JOR Spine 2019;2(1):e1047.
[27] Fearing BV, Hernandez PA, Setton LA, Chahine NO. Mechanotransduction and cell biomechanics of the intervertebral disc. JOR Spine 2018;1(3).
[28] Ghanem N, Uhl M, Muller C, Elgeti F, Pache G, Kotter E, et al. MRI and discography in traumatic intervertebral disc lesions. Eur Radiol 2006;16(11):2533–41.
[29] Li Z, Lezuo P, Pattappa G, Collin E, Alini M, Grad S, et al. Development of an ex vivo cavity model to study repair strategies in loaded intervertebral discs. Eur Spine J 2016;25(9):2898–908.
[30] Beekmans SV, Emanuel KS, Smit TH, Iannuzzi D. Stiffening of the nucleus pulposus upon axial loading of the intervertebral disc: an experimental in situ study. JOR Spine 2018;1(1):e1005.
[31] Botsford DJ, Esses SI, Ogilvie-Harris DJ. In vivo diurnal variation in intervertebral disc volume and morphology. Spine 1994;19(8):935–40.
[32] Lang G, Liu Y, Geries J, Zhou Z, Kubosch D, Sudkamp N, et al. An intervertebral disc whole organ culture system to investigate proinflammatory and degenerative disc disease condition. J Tissue Eng Regen Med 2018;12(4):e2051–61.
[33] Li Z, Lang G, Karfeld-Sulzer LS, Mader KT, Richards RG, Weber FE, et al. Heterodimeric BMP-2/7 for nucleus pulposus regeneration-In vitro and ex vivo studies. J Orthop Res 2017;35(1):51–60.
[34] Li Z, Lang G, Chen X, Sacks H, Mantzur C, Tropp U, et al. Polyurethane scaffold with in situ swelling capacity for nucleus pulposus replacement. Biomaterials 2016;84:196–209.
[35] Shu CC, Smith MM, Smith SM, Dart AJ, Little CB, Melrose J. A histopathological scheme for the quantitative scoring of intervertebral disc degeneration and the therapeutic utility of adult mesenchymal stem cells for intervertebral disc regeneration. Int J Mol Sci 2017;18(5).
[36] Caprez S, Menzel U, Li Z, Grad S, Alini M, Peroglio M. Isolation of high-quality RNA from intervertebral disc tissue via pronase predigestion and tissue pulverization. JOR Spine 2018;1(2):e1017.
[37] Farndale RW, Buttle DJ, Barrett AJ. Improved quantitation and discrimination of sulphated glycosaminoglycans by use of dimethylmethylene blue. Biochim Biophys Acta 1986;883(2):173–7.
[38] Pattappa G, Li Z, Peroglio M, Wismer N, Alini M, Grad S. Diversity of intervertebral disc cells: phenotype and function. J Anat 2012;221(6):480–96.
[39] Daly C, Ghosh P, Jenkin G, Oehme D, Goldschlager T. A review of animal models of intervertebral disc degeneration: pathophysiology, regeneration, and translation to the clinic. BioMed Res Int 2016;2016:5952165.
[40] Li Z, Kaplan KM, Wertzel A, Peroglio M, Amit B, Alini M, et al. Biomimetic fibrin-hyaluronan hydrogels for nucleus pulposus regeneration. Regen Med 2014;9(3):309–26.
[41] Haschtmann D, Stoyanov JV, Gedet P, Ferguson SJ. Vertebral endplate trauma induces disc cell apoptosis and promotes organ degeneration in vitro. Eur Spine J 2008;17(2):289–99.
[42] Dudli S, Haschtmann D, Ferguson SJ. Persistent degenerative changes in the intervertebral disc after burst fracture in an in vitro model mimicking physiological post-traumatic conditions. Eur Spine J 2015;24(9):1901–8.
[43] Dudli S, Boffa DB, Ferguson SJ, Haschtmann D. Leukocytes enhance inflammatory and catabolic degenerative changes in the intervertebral disc after endplate fracture in vitro without infiltrating the disc. Spine 2015;40(23):1799–806.
[44] Iatridis JC, MaClean JJ, Ryan DA. Mechanical damage to the intervertebral disc annulus fibrosus subjected to tensile loading. J Biomech 2005;38(3):557–65.
[45] Walter BA, Korecki CL, Purmessur D, Roughley PJ, Michalek AJ, Iatridis JC. Complex loading affects intervertebral disc mechanics and biology. Osteoarthritis Cartilage 2011;19(8):1011–8.
[46] Miyagi M, Ishikawa T, Orita S, Eguchi Y, Kamoda H, Arai G, et al. Disk injury in rats produces persistent increases in pain-related neuropeptides in dorsal root ganglia and spinal cord glia but only transient increases in inflammatory mediators: pathomechanism of chronic diskogenic low back pain. Spine 2011;36(26):2260–6.
[47] Bailey JF, Hargens AR, Cheng KK, Lotz JC. Effect of microgravity on the biomechanical properties of lumbar and caudal intervertebral discs in mice. J Biomech 2014;47(12):2983–8.
[48] Jin L, Feng G, Reames DL, Shimer AL, Shen FH, Li X. The effects of simulated microgravity on intervertebral disc degeneration. Spine J 2013;13(3):235–42.
[49] Sitte I, Kathrein A, Pfaller K, Pedross F, Roberts S. Intervertebral disc cell death in the porcine and human injured cervical spine after trauma: a histological and ultrastructural study. Spine 2009;34(2):131–40.
[50] Paul CP, Schoorl T, Zuiderbaan HA, Zandieh Doulabi B, van der Veen AJ, van de Ven PM, et al. Dynamic and static overloading induce early degenerative processes in caprine lumbar intervertebral discs. PloS One 2013;8(4):e62411.
[51] White AA, Panjabi M. Clinical biomechanics of the spine. 2nd ed. 1990. p. 106–7. ISBN 0-397-50720-8.